ACI STRUCTURAL JOURNAL TECHNICAL PAPER

Title No. 113-S52

High-Strength Reinforcement in Columns under High Shear Stresses

by Drit Sokoli and Wassim M. Ghannoum

This study investigated the performance of seismically detailed concrete columns reinforced with high-strength steel. Columns were subjected to high shear stresses and relatively high axial load to investigate the ability of high-strength reinforcement in maintaining the integrity of concrete shear-transfer mechanisms. Two columns (CS60 and CS80) were respectively reinforced with conventional Grade 60 (420 MPa) and Grade 80 (550 MPa) ASTM A706 bars. A third column, CS100, was reinforced with newly developed Grade 100 (690 MPa) bars. Columns had almost identical reinforcement layouts and flexural strengths. Shear and axial failure occurred at comparable drift levels in CS60 and CS80. CS100 sustained bond degradation around the longitudinal bars at relatively low drifts, raising questions about bar development lengths and allowable lengths of concrete members reinforced with high-strength steel. Strain demands in longitudinal and transverse bars were significantly higher in the specimens reinforced with high-strength steel.

Keywords: columns; high-strength steel; reinforced concrete; seismic.

INTRODUCTION

Current design codes place restrictive limits on the strength of reinforcing steel due to lack of test data validating adequate performance of higher strength reinforcement (for example, ACI 318-14[1] and AASHTO[2]). ACI 318-14[1] limits the yield strength of reinforcing bars to 80 ksi (550 MPa) for non-seismic systems, except when designing for shear, in which the transverse reinforcement yield strength is limited to 60 ksi (420 MPa). For seismic designs, the ACI 318-14[1] code limits yield strength of reinforcement to 60 ksi (420 MPa). Reinforcing bars with specified yield strength of 100 ksi (690 MPa) were recently allowed in the ACI 318 for confinement reinforcement.

At present, the vast majority of reinforcing steel produced and used in the United States is Grade 60 (420 MPa) (or having a specified yield strength of 60 ksi [420 MPa]). In the last decade, advances in production capabilities have resulted in reinforcing bars of Grade 80 (550 MPa) through 120 (830 MPa) with a linear preyield behavior and relatively high ductility. The newly developed reinforcing steel grades have prompted a large national effort to explore the potential introduction of such steel grades into design codes.[3-7] It should be noted that most research on high-strength steel reinforcement has been conducted in the last 15 years in Japan with SD685 steel, in Europe with SAS 670 steel, and in the United States with ASTM A1035[3] steel. The steel bars used in this experimental program have been in production for less than 5 years. The new steel rivals the mechanical properties of the Japanese SD685 steel and has different mechanical properties from ASTM A1035 steel—namely, it has higher ductility and a well-defined yield plateau.

Performance concerns that have maintained the code limits on the strength of reinforcing steel span a wide range of behavioral aspects. An increase in steel strength in reinforcing bars is associated with an increase in the strain at yield, and often with a reduction in the fracture elongation, the tensile-to-yield strength ratio, and the length of the yield plateau. For a given bar size, higher-strength steel implies larger tensile and compressive forces. Larger tensile forces for the same bar size result in an increase in bond demands and the forces at bar hooks or heads. On the other hand, larger compressive forces for the same bar size can increase bar buckling susceptibility given the same lateral bracing. The larger strain at yielding in higher-strength steel can cause larger strains at service loads and therefore increase crack widths and deflections. Larger crack widths in turn can lead to the weakening of the concrete shear-transfer mechanisms and lower shear strengths. Additionally, the lower ductility of high-strength steel may affect seismic design, member deformation capacity, as well as bar-bend performance. There is also evidence that the tensile-to-yield strength ratio affects the spread of plasticity in reinforced concrete members, and a low value of the ratio can concentrate strains in bars at cracks.

Of particular interest in this study was exploring the effects of high shear and confinement demands on the deformation capacity of concrete columns reinforced with high-strength bars. Specifically, an experimental program was undertaken to investigate the ability of high-strength reinforcing bars (HSRB) to maintain the integrity of shear transfer mechanisms at large deformation demands during seismic events. As large shear stresses coupled with the use of high-strength reinforcing bars generate large bond demands between longitudinal bars and concrete, the effects of increased bond demands generated were also investigated. In this study, high-strength steel refers to reinforcing steel having yield strength of 80 ksi (550 MPa) or more.

Three full-scale concrete columns reinforced with bars having variable steel grades were tested to residual lateral strength or collapse. Columns had almost identical reinforcement layouts and flexural strengths. Columns were designed to impart large demands on transverse reinforcing bars through high shear stresses and confinement demands. Columns were subjected to relatively large shear stresses generated by high longitudinal reinforcement ratios.

ACI Structural Journal, V. 113, No. 3, May-June 2016.

MS No. S-2015-132.R1, doi: 10.14359/51688203, was received May 5, 2015, and reviewed under Institute publication policies.

Confinement demands were generated by a relatively high compressive axial load.

RESEARCH SIGNIFICANCE

Design standards limit the use of HSRB in seismic and shear applications. Uncertainty about the effects of HSRB on deformation capacity and the integrity of shear transfer mechanisms has sustained the restrictions. Recent advances in production techniques have delivered HSRB having a linear pre-yield behavior and relatively high ductility. This study is the first to compare the cyclic behavior of full-scale columns reinforced using Grade 60 A706 bars and the newly developed higher Grades 80, 100, and 120 bars. The study focused on the effects of high shear, bond, and confinement demands on the deformation capacity of concrete columns with HSRB.

EXPERIMENTAL INVESTIGATION

Three geometrically identical columns were tested under constant compressive axial load and quasi-static reversed cyclic lateral loading until loss of axial strength or residual lateral strength. Column CS60 was reinforced exclusively with Grade 60 ASTM A706 bars. Column CS80 was reinforced exclusively with Grade 80 A706 bars, and Column CS100 was reinforced with newly developed Grade 100 longitudinal bars and Grade 120 transverse hoops. Columns satisfied most of the seismic provisions for special moment frames of ACI 318-14.[1] The imposed shear stresses resulted in a design with the shear contribution of transverse reinforcement exceeding the $8\sqrt{f_c'}$ (psi units) ($0.67\sqrt{f_c'}$ [MPa units]) limit imposed by ACI 318-14; where f_c' is concrete compressive strength. In addition, the hoop spacing in CS60 and CS80 exceeded by 1 in. (25.4 mm) the maximum allowed spacing in ACI 318-14 for confinement of plastic hinge regions. All columns were designed to have almost identical flexural capacity and associated shear demands. The hoop spacing limits of ACI 318-14 were met in Column CS100.

Specimen detailing

All three columns were designed with a target concrete compressive strength of 4.5 ksi (31 MPa). Investigating the interaction of HSRB with high-strength concrete was not within the scope of this study. Reinforcement details for column specimens are given in Fig. 1 and Table 1. The shear span-depth ratio (a/d) was approximately 2.7 for all columns (refer to Notation for term definitions). For CS60 and CS80, the longitudinal bars were anchored in footings using standard ACI 318-14[1] hooks. In CS100, headed bars were used for ease of construction. Columns did not contain any lap splices. Transverse bars in all specimens satisfied the ACI 318-14[1] definition for hoops and were bent to current ACI 318-14[1] bend radii.

Sectional analyses were performed at the design stage and accounted for a compressive axial load of 370 kip (1646 kN). Given the target concrete compressive strength of 4.5 ksi (31 MPa), the resulting design axial load ratio was 27% of $A_g f_c'$, where A_g is the gross sectional area). The expected plastic moment strength (M_{pr}) for all three columns was approximately 7500 kip-in. (847 kN-m), which resulted in a corresponding peak shear demand V_e of 178 kip (792 kN).

Table 1—Specimen reinforcement summary

	CS60	CS80	CS100
Longitudinal reinforcement	No. 10 (32 mm) ρ_l = 4.7%	No. 9 (29 mm) ρ_l = 3.7%	No. 8 (25 mm) ρ_l = 2.9%
Transverse reinforcement	No. 5 (16 mm) at 5.5 in. (140 mm) $4.4d_b$ ρ_t = 1.50%	No. 4 (13 mm) at 5.5 in. (140 mm) $4.9d_b$ ρ_t = 0.94%	No. 3 (10 mm) at 4.5 in. (114 mm) $4.5d_b$ ρ_t = 0.65%

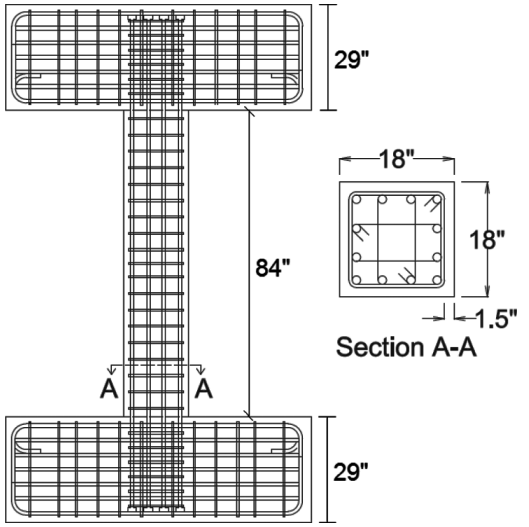

Fig. 1—Vertical section of column specimens. (Note: 1 in. = 25.4 mm.)

The expected peak shear stress (V_e/bd) was therefore $9.6\sqrt{f_c'}$ (psi) ($0.8\sqrt{f_c'}$ [MPa]) for all columns. As flexural yielding was intended in the tests, the shear strength of the column was designed to be larger than V_e/ϕ (with $\phi = 0.75$ as per ACI 318-14). Therefore, the steel contribution to shear strength V_s exceeded the ACI 318-14 limit of $8\sqrt{f_c'}$ (psi) ($0.67\sqrt{f_c'}$ [MPa]) and was, in all cases, approximately equal to $10\sqrt{f_c'}$ (psi) ($0.83\sqrt{f_c'}$ [MPa]). The imposed maximum shear stress was selected such that hoop design was governed by shear and not confinement requirements. ACI 318-14 limits the transverse hoop spacing in plastic hinge regions to one-fourth of the smallest column dimension for confinement, which is equal to 4.5 in. (110 mm) for all specimens. In Columns CS60 and CS80, the provided hoop spacing exceeded that limit by 1 in. (25.4 mm), while it was met in CS100.

Test setup and instrumentation

The full-scale specimens were tested under symmetric double curvature with fixed rotation boundary conditions at the top and bottom. The I-shaped specimens (Fig. 2) were prestressed to the strong floor and steel reaction frame using threaded rods. Two vertical actuators (Fig. 2) applied a constant compressive axial load during testing that was adjusted for large deformation equilibrium during the tests. The resulting compressive axial load on columns, including the self-weight of the specimens and apparatus, was 370 kip (1646 kN). The lateral loading protocol imposed by the horizontal actuator to all three columns consisted of two fully reversed lateral drift cycles at increasing target drifts as per FEMA 461[8] recommendations. The targeted lateral

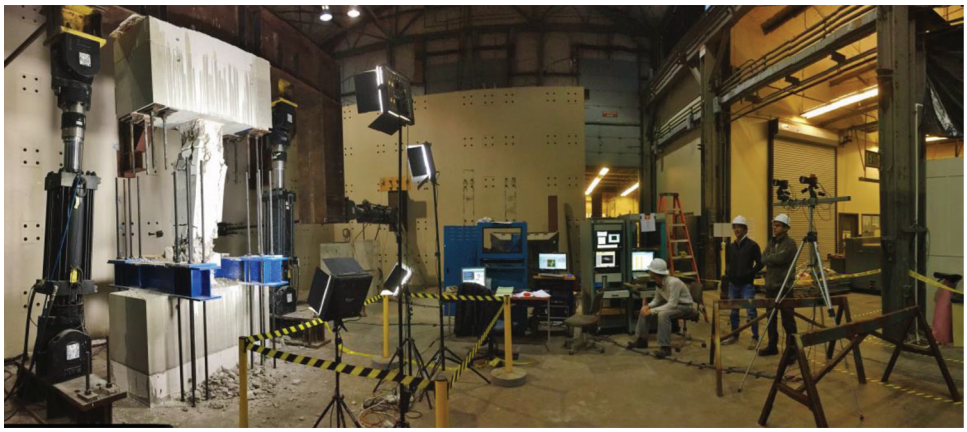

Fig. 2—Column CS100 and test setup at end of test.

drift ratios (that is, the ratios of lateral drifts to column clear height) were: 0.2, 0.3, 0.4, 0.6, 0.8, 1.0, 1.5, 2.0, 3.0, 4.0, 5.5, and 7.0%. Tests were carried in displacement control under small loading rates.

Columns were instrumented to measure the applied loads, distributed surface deformations, and reinforcing bars' strains. A digital image correlation (DIC) system developed by the authors was used to measure column surface deformations, from which surface strains and crack widths were obtained.[9] The DIC system was able to resolve column deformations on the order of 1/10,000 of an inch (1/400 of 1 mm) over the field of view. Column deformations were obtained at targets placed in a regular 2.75 x 2.75 in. (70 x 70 mm) grid over the surface of columns (Fig. 3). Strain gauges were installed on transverse hoops within the top and bottom plastic hinge regions. Eight strain gauges were affixed to the four corner longitudinal bars at the interfaces with the top and bottom footings, where bar strain demands were expected to be highest.

Material properties

Concrete strength was measured at the day of column testing using three cylinders per ASTM C39.[10] The three-cylinder average concrete compressive strength was 3.83 ksi (26.4 MPa) for CS60, 4.18 ksi (28.8 MPa) for CS80, and 4.65 psi (32 MPa) for CS100. Reinforcing steel coupons were taken from the same heat as the steel used in each specimen. Three steel coupons per bar type and grade were tested monotonically in tension to fracture as per ASTM A370.[11] Table 2 summarizes the three-coupon average material properties for each steel grade and bar size. The uniform elongations presented in Table 2 are defined as the strains at peak stress and were calculated in accordance with ASTM E8.[12] Figure 4 presents typical stress-strain relations for the bars used in the columns. All steel stress-strain curves had a similar shape, with nearly linear behavior up to yielding and a well-defined yield plateau. The tensile-to-yield strength ratios (T/Y) gradually decreased as the yield strength increased and ranged from 1.41 for No. 10 (32 mm) Grade 60 bars to 1.18 for No. 3 (10 mm) Grade 120 bars (Table 2). Likewise, the fracture and uniform elongations decreased with increasing yield strength. The higher-grade bars did, however, achieve relatively high uniform elongations that were at most 20% lower than those for Grade 60 bars.

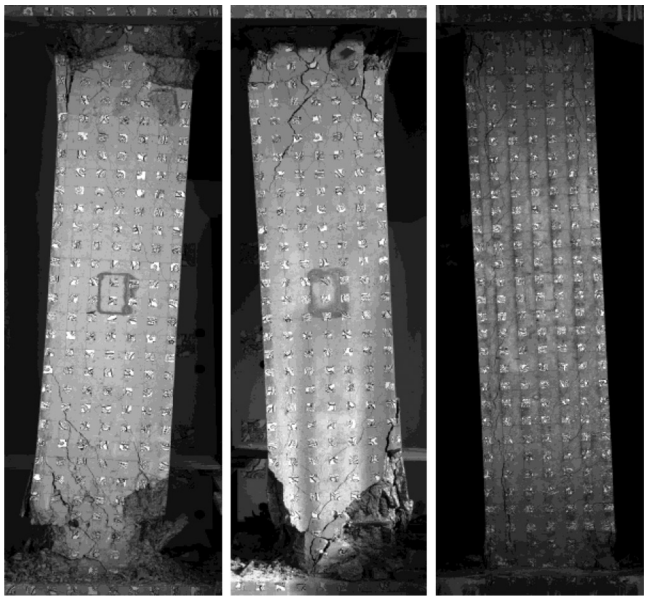

Fig. 3—Specimens just prior to initiation of lateral strength loss (left to right: CS60, CS80, and CS100).

Data processing

All reported column deformations were gathered using the DIC system. Target displacement data from the DIC system were used to calculate rotations, curvatures, and deformation components at each row of targets over the height of the specimens, as described in Sokoli et al.[9] Curvature profiles along column length were evaluated by calculating the curvature between adjacent horizontal target rows as the difference in angle of rotation between the two rows divided by the measured distance between them. Flexural deformations were extracted from target displacement values by integrating those curvatures over the height of the column. Shear deformations were evaluated as the difference in lateral displacement between successive rows of targets after subtracting the flexural deformation. The slip of longitudinal bars from adjacent members causes rigid body rotation of a column about the interface between the column and adjacent members, which was measured using the DIC

Table 2—Average steel material properties from coupon tension tests

Bar size (mm)	Grade	Yield strength, ksi (MPa)	Tensile strength, ksi (MPa)	Tensile-to-yield ratio	Yield strain	Fracture elongation, %	Uniform elongation, %
No. 10 (32)	60	67.3 (464)	94.9 (654)	1.41	0.0022	18.3	10.1
No. 9 (29)	80	79.1 (545)	106.5 (734)	1.34	0.0025	15.5	8.8
No. 8 (25)	100	101.5 (700)	128.5 (886)	1.26	0.0035	11.6	8.3
No. 5 (16)	60	68.5 (472)	95.8 (660)	1.40	0.0022	14.4	9.9
No. 4 (13)	80	83.7 (577)	111.4 (768)	1.33	0.0030	12.1	8.9
No. 3 (10)	120	118.9 (820)	141.0 (972)	1.18	0.0041	10.1	8.4

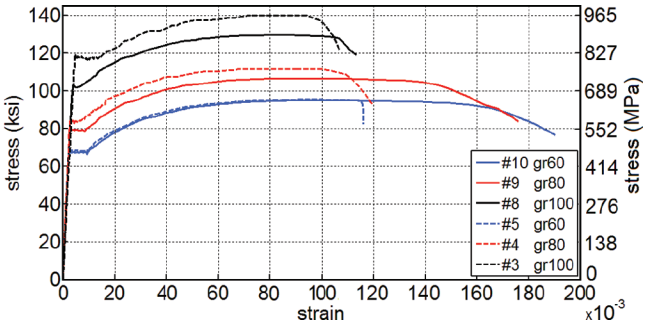

Fig. 4—Typical reinforcement stress-strain curves.

system.[9] The surface targets arranged in a rectangular mesh were used as nodal points for bilinear-strain quadrilateral elements (Fig. 3). By assuming that strains varied linearly between targets, the following element strains were calculated for each quadrilateral element: the x-directional, or horizontal, strains ε_x; the y-directional, or vertical, strains ε_y; and the principal strains (ε_1 = largest principal strain and ε_2 = smallest principal strain). Figure 5 illustrates the x-direction surface strain measurements for CS100 at various target drifts. As can be seen in the figure, cracks and the locations of concrete spalling are clearly visible in the strain readings.

At inclined crack locations and the peak of each drift excursion, the horizontal strain measurements from the DIC system match reasonably well the strains measured by strain gauges on the hoops.[9] Because inclined cracks rarely crossed hoop strain gauges, peak strain demands on the hoops were estimated using the DIC system.

Applied column forces and moments were computed using large-deformation equilibrium accounting for the location and inclination of all three actuators.

COLUMN BEHAVIOR

Overall behavior

Behavioral and damage milestones for the columns are summarized in Table 3 and identified on the column lateral load *V* versus lateral drift ratio relations in Fig. 6 to 8.

Columns CS60 and CS80 showed comparable response up to initiation of lateral strength loss, which occurred beyond the second excursion to a drift ratio of +5.5%. Column CS60 initiated loss of lateral strength immediately prior to loss of axial capacity at a drift ratio of +5.2% as the column was being pushed to the first excursion to a drift ratio of +7.0% (Fig. 6). The initiation of lateral-strength loss in CS80 occurred just prior to loss of axial capacity at a drift ratio of –4.6% as the column was being pushed to the first excursion to a drift ratio of –7.0% (Fig. 7). For both columns, axial collapse occurred when the shear-damaged area could no longer sustain the imposed axial load and vertical sliding occurred across the critical inclined cracks. Column CS60 started losing axial capacity at a drift ratio of +5.8% while CS80 initiated axial failure at a drift ratio of –5.5%. Beyond the initiation of axial failure (IAF), column axial loads were reduced gradually to 280 kip (1248 kN) for CS60 and 230 kip (1023 kN) for CS80 as they were pushed monotonically to a drift ratio of +9.1% for CS60 and –8.2% for CS80. In both specimens, even considering that the concrete cover spalled off over wide regions at both ends, no buckling was observed in the longitudinal reinforcement up to the initiation of axial failure. Images of columns soon after the initiation of lateral-strength loss are shown in Fig. 3. No bar fracture was observed in either CS60 or CS80 at the end of the tests.

A stable response up to a drift ratio of 4% is generally considered to be a minimum performance objective for collapse prevention at the maximum considered earthquake (MCE) hazard level. Both CS60 and CS80 showed comparable lateral load behavior and remained stable beyond two cycles at a drift ratio of 5.5% (Fig. 8). Mechanical properties of the reinforcement did not dictate major differences between the behaviors of the two specimens. Grade 80 reinforcement preserved the integrity of the concrete core and shear transfer mechanisms to the same high demand levels as the conventional Grade 60 reinforcement.

Column CS100 showed a comparable behavior to Columns CS60 and CS80 up to a drift ratio of 1.5% (Fig. 9). The crack pattern in the CS100 was similar to those of the other two columns until the end of the 1.5% drift cycles. Figure 5 indicates an increase in the horizontal (x-direction) strains along the outmost longitudinal bars at column ends during the first cycle to a drift ratio of –2.0%. These strains corresponded to longitudinal hairline cracks that formed in the plastic hinge regions at the location of the outer longitudinal bars. At the end of first cycle toward a drift ratio of –3.0% (Fig. 5), severe longitudinal cracks spread over the height of the column and were associated with bond degradation at the longitudinal bars. The initiation of lateral strength loss occurred at this drift ratio of –3.0%, beyond which column lateral strength dropped significantly. The column was cycled up to and through the 5.5% drift cycles, as its lateral strength dropped to 32 kip (142 kN)—18.9% of peak strength. The column was then pushed monotonically to a drift ratio of +12% drift without loss of axial strength, while the lateral strength

Table 3—Behavioral milestones for each specimen

	CS60		CS80		CS100	
	V, kip (kN)	Drift ratio, %	*V*, kip (kN)	Drift ratio, %	*V*, kip (kN)	Drift ratio, %
First longitudinal reinforcement yield	164 (730)	1.60	148 (658)	1.00	150 (667)	1.23
First transverse reinforcement yield	159 (707)	3.10	–170 (–756)	–2.00	–98 (–436)	4.00
First flexural crack	–76 (–338)	–0.30	98 (436)	0.40	–85 (–378)	–0.40
First inclined crack	104 (462)	0.60	101 (449)	0.60	103 (458)	0.60
Peak lateral load	176 (782)	2.90	178 (792)	1.90	169 (752)	2.00
Initiation of lateral strength loss	144 (640)*	5.20*	–150 (–667)*	–4.60*	158 (702)†	–3.00†
Initiation of axial failure	135 (601)	5.80	–112 (–498)	–5.50	NA	12.00‡

*Initiation of lateral strength loss due to shear strength degradation.

†Initiation of lateral strength loss due to bond degradation.

‡Test was stopped at actuator displacement limit.

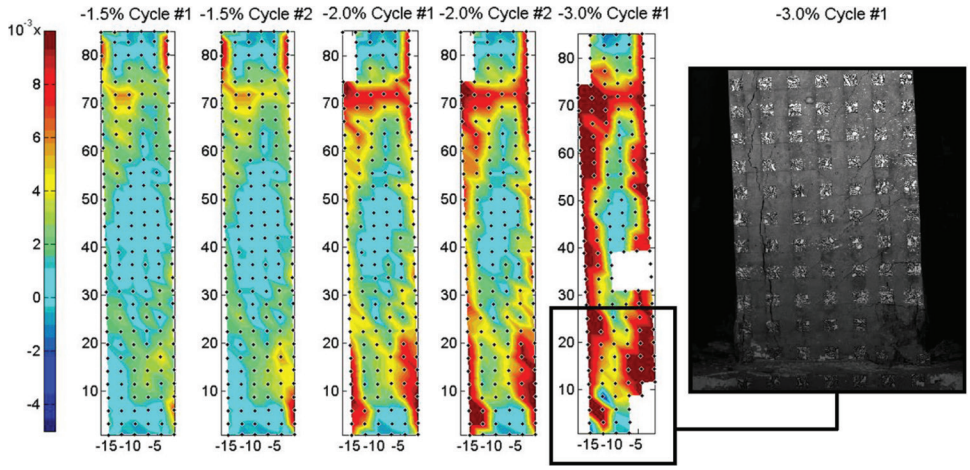

Fig. 5—Horizontal (x-direction) strains for CS100 at selected target drift ratios. Blank areas represent loss of targets and positive values indicate tension strains. (Note: 1 in. = 25.4 mm.)

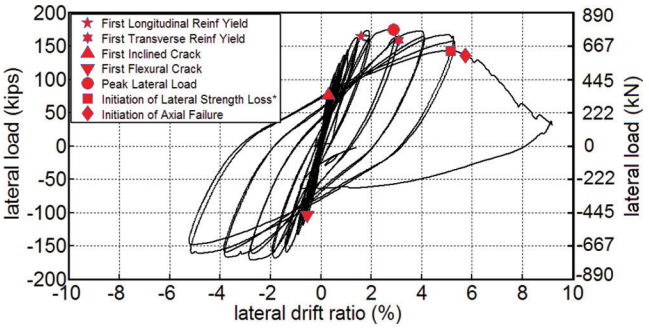

Fig. 6—Lateral load-versus-drift ratio response of CS60.

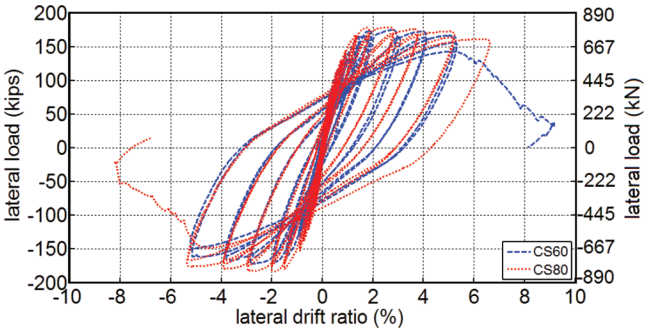

Fig. 8—Comparison of lateral load-versus-drift response comparison of CS60 and CS80.

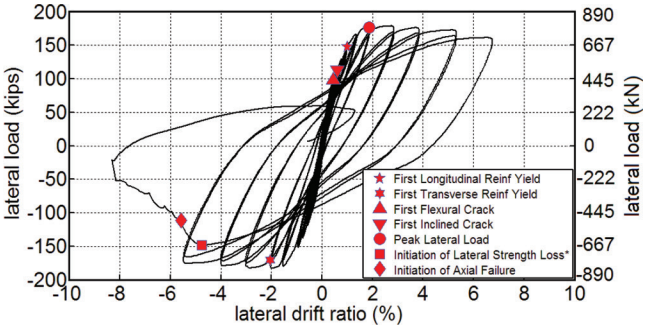

Fig. 7—Lateral load-versus-drift ratio response of CS80.

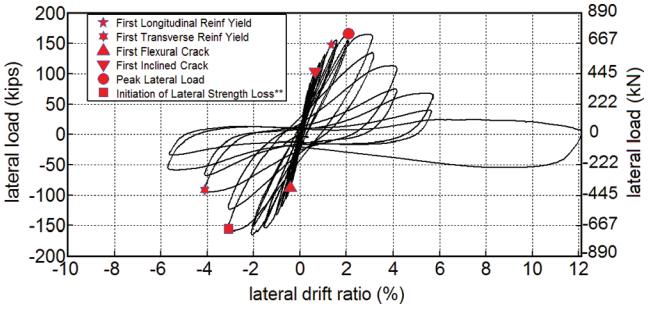

Fig. 9—Lateral load-versus-drift ratio response of CS100.

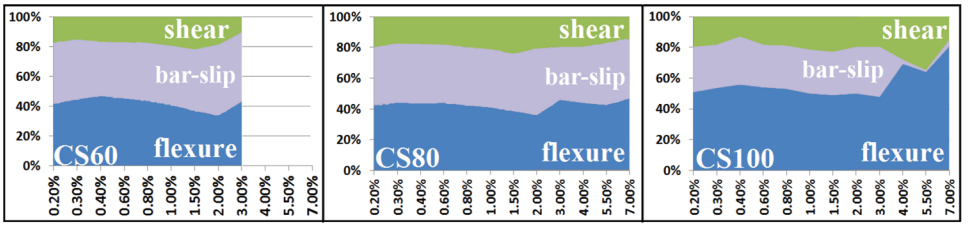

Fig. 10—Deformation components at first excursion to drift targets.

dropped to 13 kip (58 kN)—7.7% of peak lateral strength. The bond splitting failure released longitudinal bar stresses as well as the imposed shear forces on the column, which prevented the concrete core from sustaining the shear/axial failure mode observed in the other two columns.

Deformation components

Column lateral deformation at the top footing interface was deconstructed into three components: flexural, shear, and bar-slip deformations. Typically, shear deformations in concrete columns comprise approximately 5% of the total deformations, but can be more significant in shorter columns.[13] Flexural deformations typically comprise 40 to 60% of the total, while bar-slip induced deformations can comprise up to 40% of the total.[14,15]

The deformation components of each specimen are shown as a fraction of column total lateral drifts in Fig. 10. For CS60, DIC data were unreliable beyond the drift cycles to 3.0% and are not reported. Columns CS60 and CS80 showed similar distributions of deformation components. Shear deformations were similar for all three columns from the beginning of tests to a drift ratio of 3.0%. In all columns, shear deformations accounted for approximately 20% of column drifts from low deformation levels up to the initiation of lateral strength loss. The large contributions of shear deformations were due to the high column shear stresses. Test results therefore indicate that shear deformations should not be ignored in analyses when shear stresses are large. Column CS100 experienced slightly larger flexural deformations than other columns at any particular drift level. Beyond a drift ratio of 3.0%, bar-slip deformations in CS100 die out due to the release of longitudinal bar stresses caused by bond failure.

DEMANDS ON BARS

Demands on longitudinal bars

The maximum strain gauge measurements from all longitudinal bar gauges are plotted at each drift target for each column in Fig. 11. The No. 10 (32 mm) Grade 60 bars used as longitudinal reinforcement in CS60 had an average yield strain of 0.0023 as measured from coupon tests. This strain was reached at a drift ratio of +1.6% in the first cycle toward a drift target of 2.0%. The No. 9 (29 mm) Grade 80 bars used as longitudinal reinforcement in CS80 had an average measured yield strain of 0.0027. This strain was achieved at the end of the first cycle toward a drift ratio of 1.0%. The longitudinal bars in CS100 reached their average yield strain of 0.0035 at the end of the first cycle toward a drift ratio of 1.0%. As can be seen Fig. 11, the Grade 80 longitudinal bars in CS80 saw significantly larger strains at all drift levels, and were up to 65% higher, than those in longitudinal bars of CS60. Owing to

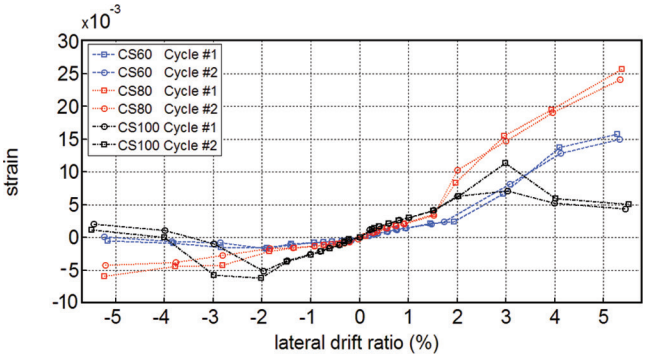

Fig. 11—Maximum measured strains in longitudinal reinforcement at target drift ratios.

the lower fracture strains of the higher-grade bars, the longitudinal bars in CS80 reached 16.4% of their fracture strain at the end of the drift cycles to 5.5%, whereas longitudinal bars in CS60 only reached 8.7% of their fracture strain. The longitudinal bars in CS100 did not reach as high strains as those in the other two columns due to the premature bond-splitting failure. However, longitudinal bars in CS100 had significantly higher strains (approximately 25% higher than in CS80 and 100% higher than in CS60) up to the end of the 1.5% drift cycles and prior to significant loss of bond (Fig. 11).

The low-cycle fatigue behavior of reinforcing bars is highly dependent on the strain amplitudes the bars experience. A 100% increase in strain amplitudes can lead to an order of magnitude reduction in the number of cycles-to-fracture of reinforcing bars.[16,17] The recorded strain amplitudes in the longitudinal bars of the tested columns were relatively low owing to the relatively high axial load. However, the observed larger strains in the HSRB compared with Grade 60 bars raises the concern that HSRB may fracture prematurely compared with Grade 60 counterparts in applications where large strain amplitudes are expected (for example, concrete columns or walls with low axial loads).

Demands on transverse bars

Measurements of hoop strains obtained from the DIC system at inclined crack locations are presented in Fig. 12. Strain measurements are only provided in the figures up to the first drift ratio excursion to 3.0%, beyond which damage in the columns rendered strain measurements unreliable.

At a drift ratio of 3.0%, hoops in CS80 reached a peak strain of 1.6%, while hoops in CS100 reached a similar peak strain of 1.4%. Hoops in CS60, on the other hand, reached a lower maximum strain of 1.1%. Columns reinforced with higher-grade bars (CS80 and CS100) therefore experienced up to 45% higher hoop strains than the column reinforced with Grade 60 bars (CS60).

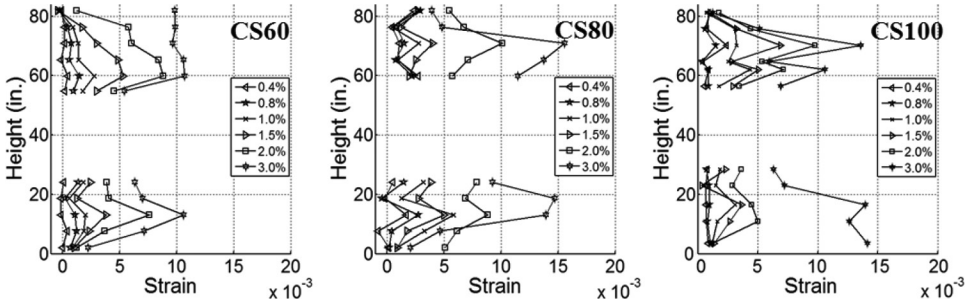

Fig. 12—Maximum estimated hoop strains at column ends. (Note: 1 in. = 25.4 mm.)

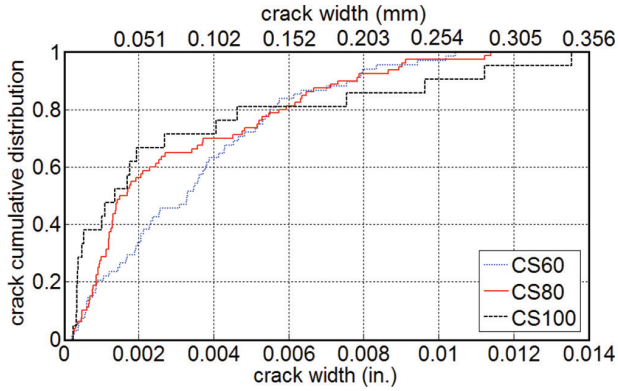

Fig. 13—Cumulative distribution plot for inclined cracks at 70% V_{max}.

CRACKING

A concrete crack was assumed to have formed when the largest principal tensile strain (ε_1) within a quadrilateral element formed by four surface targets exceeded an assumed cracking strain, $\varepsilon_{cr} = f_t'/E_c = 7.5/57{,}000 = 1.3 \times 10^{-4}$. After an initial crack formed in an element, the average elastic strain in the adjacent uncracked concrete was assumed to be half the cracking strain. Thus, the crack width within a surface element was calculated by subtracting half the cracking strain from the largest principal tensile strain and then multiplying the modified strain by the surface element's equivalent length taken as the diameter of a circle of equivalent area to the square element.

Little difference in the widths of flexural cracks was noted between all three specimens. At 70% of the maximum recorded shear load V_{max}, flexural crack widths were similar for all three columns, with the CS100 having the widest cracks that were, on average, 16% wider than those in CS80 and 14% wider than those in CS60. The flexural crack widths in all columns at this loading stage were smaller than 0.01 in. (0.254 mm), owing to the relatively high axial load.

The cumulative distribution of the inclined crack widths are reported at 70% V_{max} in Fig. 13. Inclined cracks were defined as cracks having an angle between 25 and 65 degrees based on the angle of principal strain ε_1 from the horizontal line. At that loading stage, Column CS100 had a few inclined cracks that were wider than the widest cracks in CS60 and CS80. These wider cracks in CS100 concentrated deformations, resulting in other cracks in CS100 being on average narrower than those in CS60 and CS80.

MODES OF DEGRADATION

Shear

An increase in lateral deformations, particularly inelastic deformations, decreases the shear strength in reinforced concrete columns.[14,18] As the plastic hinge is pushed to large rotations and transverse reinforcement to higher strains, inclined cracks tend to widen, thereby reducing the effectiveness of shear transfer mechanisms. In columns with slightly greater design shear strength than shear demands generated by the plastic moment capacity, shear failure can occur after inelastic deformations in the plastic hinges reduce shear strength sufficiently. In such cases, columns can undergo relatively large inelastic deformation prior to shear failure.

Columns CS60 and CS80 sustained relatively large inelastic deformations prior to sustaining shear and axial strength degradations. Crushing and sliding across the critical inclined cracks caused the shear and axial failures. Even though strains were higher in Grade 80 hoops than in Grade 60 hoops, test results demonstrated the effectiveness of Grade 80 hoops in preserving the integrity of core concrete as CS80 was pushed beyond a drift ratio of 5.5% under relatively large axial load and high shear stresses.

The shear stresses in the column specimens were high, such that the steel contribution to shear strength evaluated according to ACI 318-14 (V_s) was $10\sqrt{f_c'}$ (psi) ($0.83\sqrt{f_c'}$ [MPa]), which is larger than the $8\sqrt{f_c'}$ (psi) ($0.67\sqrt{f_c'}$ [MPa]) limit in ACI 318-14. Given the relatively large deformation capacities observed of columns CS60 and CS80, it may be warranted to increase the limit on the shear stress contribution of transverse reinforcement imposed by ACI 318-14 to $10\sqrt{f_c'}$ (psi) ($0.83\sqrt{f_c'}$ [MPa]) for well-confined frame members.

It is noteworthy that shear and axial degradations occurred almost simultaneously in these columns, which is corroborated by findings of a study by LeBorgne and Ghannoum.[19] In that study, once loss of shear strength initiated, the degradation of the shear-resisting mechanism leading to axial collapse was noted to occur at lower drifts for columns with higher transverse reinforcement ratios and axial loads. Columns that contain relatively high transverse reinforcement ratios tend to sustain shear failures through crushing of the concrete core as opposed to diagonal tension and yielding of the transverse reinforcement. Compressive axial loads further exacerbate the core failure mechanism.

ASCE 41-13[20] provides estimates of the plastic rotation capacities of concrete columns given column shear and flexural strengths, peak shear stress, transverse reinforcement

Table 4—Plastic rotations at shear and axial failure, rad

		ASCE 41-13	Test data*
CS60	a†	0.025	0.041
	b†	0.040	0.048
CS80	a	0.019	0.042
	b	0.042	0.046

*Test data represent plastic rotation over assumed plastic hinge length of *h,* including bar-slip.

†"a" is rotation at initiation of lateral strength loss; and "b" is rotation at axial failure.

ratios, and axial loads. Table 4 summarizes the plastic rotations at: a) shear failure; and b) axial failure, as estimated using ASCE 41-13. Table 4 also summarizes the plastic rotation values measured using the DIC system at the base of the columns where shear and axial failures occurred. Column-end rotations were obtained as the difference in rotation between the row of targets 18 in. (458 mm) from the base of the columns and the row of targets on the bottom footings. Plastic rotations were obtained by subtracting column-end rotations at first yield from the maximum rotations reached prior to initiation of shear and axial strength degradation. The measured rotation quantities include the bar-slip component.

As can be seen in Table 4, ASCE 41-13 underestimates the plastic rotation at shear failure for both columns but is in reasonable agreement with the rotations at axial failure. It is noteworthy that the ASCE 41-13 plastic rotation estimates at shear failure were substantially lower than those at axial failure, unlike what was observed in the column tests where axial failure occurred shortly after shear failure.

Bond

The high shear stresses in the columns generated steep moment gradients and relatively high bond demands on the longitudinal bars. The columns were designed such that the increase in bar yield strength from CS60 to CS80 and CS100 was offset by a reduction in bar diameter, which resulted in a nearly identical longitudinal bar force across grades ($F_b = A_s f_y$, where A_s is the total area of longitudinal reinforcement and f_y is the measured yield strength). However, by balancing the forces in the longitudinal bars of differing strengths, the bond demands at the bar surface were increased with increasing bar strength and required a longer development length (l_d). The provided development length, on the other hand, remained constant, as all columns had the same clear length.

Columns CS60 and CS80 did not show any signs of bond deterioration. In Column CS100, longitudinal cracks formed in the concrete cover along the corner longitudinal bars within the plastic hinge regions at a drift ratio of 1.5% (Fig. 5). The cracks formed after flexural yielding occurred and the peak flexural strength was reached. At a drift ratio of 1.5%, however, lateral strength was maintained despite the apparent longitudinal splitting cracks. During subsequent reversed cyclic loading, the splitting cracks propagated over the height of the member. Once the splitting planes propagated far enough along column height, lateral strength loss initiated during the second cycle toward a drift ratio of +3.0%. The splitting bond failure caused

Table 5—Development length equations of ACI 318-14 and ACI 408R-03

ACI 318-14	ACI 408R-03
$l_d = \frac{3}{40}\frac{f_y}{\lambda\sqrt{f'_c}}\frac{\psi_t\psi_e\psi_s}{\frac{c_b + K_{tr}}{d_b}}d_b$	$l_d = \frac{\left(\frac{f_y}{f'^{\frac{1}{4}}_c} - 2400\phi w\right)\lambda}{76.3\phi\left(\frac{cw + K_{tr}}{d_b}\right)}d_b$
Transverse reinforcement confinement term $\frac{c_b + K_{tr}}{d_b} \le 2.5$ $K_{tr} = \frac{40A_{tr}}{sn}$	Transverse reinforcement confinement term $\frac{cw + K_{tr}}{d_b} \le 4.0$ $K_{tr} = \frac{0.5A_{tr}t_d}{sn}\sqrt{f'_c}$

permanent degradation in the strength and stiffness of the column (Fig. 5 and 9), as well as a reduction in longitudinal bar stresses and strains, which unloaded due to lack of bond with the concrete (Fig. 11). The maximum strain measured in the longitudinal reinforcement of the CS100 specimen at the time of lateral strength loss was equal to the strain corresponding to the end of the yield plateau.

The lengths required to develop the strength of longitudinal bars were evaluated in accordance with ACI 318-14[1] and ACI 408R-03[21] (Table 5). Both development length equations in Table 5 contain a transverse reinforcement confinement term. ACI 318-14[1] limits the confinement term to 2.5, beyond which adding more transverse reinforcement does not reduce the required development length, and a bar pullout failure mode is assumed. ACI 408R-03,[18] on the other hand, allows a higher amount of transverse reinforcement to be accounted for in the confinement term before reaching the cap on the term. For all columns tested, the confinement term is to be capped at 2.5 according to the ACI 318-14 provisions, whereas using ACI 408R-03, none of the column transverse reinforcement layouts triggered the limit on the confinement term. Development-length values presented in Table 6 were evaluated using measured steel yield strengths and concrete compressive strengths. Because the ACI 318-14 relations provide a length to develop $1.25f_{yspec}$, the development lengths obtained using the ACI 318 relations were adjusted by the ratio $f_{smax}/1.25f_{yspec}$ (with f_{smax} being the maximum measured stress during a test in longitudinal bars). When using the development length relations of ACI 408R-03, the ϕ factor of 0.82 was omitted. For ACI 318-14 relations, development length values are provided with various limits on the confinement term: 1) the current ACI 318-14 limit of 2.5 ($l_{d\text{-}318\text{-}1}$); 2) the limit increased to 3.0 ($l_{d\text{-}318\text{-}2}$); and 3) the confinement term unlimited ($l_{d\text{-}318\text{-}3}$). As can be seen in Table 6, ACI 318-14 relations produce longer required development lengths than those available for all columns when the confinement term is capped at 2.5. According to these values, all columns should have sustained bond failures. Because CS60 and CS80 did not sustain bond failures, ACI 318 relations are conservative for those columns. Column CS100 failed by bond splitting only after significant spalling at column ends reduced the available development length from a column half-height of

Table 6—Development length calculations according to ACI 318-14 and ACI 408R-03

	Available development length, in. (mm)	ACI 318-14				ACI 408R-03	
		Confinement term $\frac{c_b + K_{tr}}{d_b}$	$l_{d\text{-}318\text{-}1}$, in. (mm)	$l_{d\text{-}318\text{-}2}$, in. (mm)	$l_{d\text{-}318\text{-}3}$, in. (mm)	Confinement term $K_{tr} = \frac{0.5A_{tr}t_d}{sn}\sqrt{f'_c}$	$l_{d\text{-}408}$, in. (mm)
			Confinement term limited to 2.5	Confinement term limited to 3	Confinement term unlimited		Confinement term limited to 4.0
CS60	33.00 (838)	3.45	33.44 (849)	27.87 (708)	24.25 (616)	3.38	30.90 (785)
CS80	31.70 (805)	3.18	36.20 (919)	30.17 (766)	28.46 (722)	2.98	41.50 (1054)
CS100	31.70 (805)	3.19	36.78 (934)	30.65 (779)	28.81 (732)	2.85	47.15 (1198)

42 in. to 31.7 in. (1067 mm to 805 mm). Because $l_{d\text{-}318\text{-}1}$ for CS100 is 36.2 in. (919.5 mm), the ACI 318 relations in their current form are conservative for Column CS100. If the cap of 2.5 on the transverse reinforcement confinement term is removed in the ACI 318 relations, the resulting development lengths indicate that all columns should have a sufficient development length to preclude a bond failure, which was not the case for CS100. Increasing the cap to 3.0, however, led to CS100 having a required development length that is almost identical to the development length available at bond failure. Estimated development lengths using ACI 408R-03 ($l_{d\text{-}408}$) were conservative for Column CS100. The $l_{d\text{-}408}$ values were significantly larger and more conservative than $l_{d\text{-}318\text{-}1}$ values for CS80 and CS100.

To preclude bond failure in concrete columns, especially those reinforced with high-strength bars, an explicit check on the development length of longitudinal bars should be performed. The ACI 318-14 development length equations can be conservatively used for this check. For well-confined columns satisfying ACI 318-14 special moment frame (SMR) provisions, an increase on the cap of the confinement term from 2.5 to 3.0 may be applied, as indicated by test results. The calculated minimum required development length should be checked against an effective available development length. Based on the measured extent of spalling in column tests, the effective available development length for longitudinal reinforcing bars in well-confined concrete columns sustaining inelastic deformations in their plastic hinge regions should not be taken larger than $((l/2) - (2/3)d)$, where l is the clear span of the member. This limit on development length results in an effective available development length of 31.7 in. (805 mm) for the tested columns, which is in close agreement with measured values presented in Table 6 and with recommendations by Ichinose.[22]

SUMMARY AND CONCLUSIONS

Three full-scale columns reinforced with varying steel grades were tested under cyclic lateral loading and high shear and axial stresses. Column CS60 was reinforced exclusively with Grade 60 ASTM A706 bars. Column CS80 was reinforced exclusively with Grade 80 A706 bars, while column CS100 was reinforced with newly developed Grade 100 longitudinal bars and Grade 120 transverse hoops. All columns were designed to have almost identical bar layouts, flexural capacity, and associated shear demands. The study focused on the effects of high shear, bond, and confinement demands on the deformation capacity of concrete columns with high-strength reinforcing bars (HSRBs). The following main observations and conclusions were made:

- Columns CS60 and CS80 showed comparable lateral load behavior and remained stable beyond two fully reversed cycles at a lateral drift ratio of 5.5%. The lateral load-versus-drift response was very similar for both columns.
- Both CS60 and CS80 sustained shear and axial failures at approximately the same relatively high drift level. Test results therefore indicate that Grade 80 (550 MPa) A706 reinforcement maintained the integrity of the shear transfer mechanisms as well as Grade 60 (420 MPa) A706 reinforcement.
- No buckling of longitudinal bars was observed up to severe damage with ratios of hoop spacing to longitudinal bar diameter s/d_b = 4.5 for CS100 and 4.9 for CS80. ACI 318-14 requires the ratio of hoop spacing to longitudinal bar diameter (s/d_b) not to exceed 6. This limit applies to members reinforced with Grade 60 steel. Test results therefore indicate that a hoop spacing of 4.5 to 5 times the longitudinal bar diameter may be acceptable for the seismic design of concrete columns reinforced with higher-strength steel.
- At the end of all tests and after severe strength loss, no bar fractures were reported in any column, even though hoops of all steel grades were bent to current ACI 318-14 bend radii.
- Longitudinal bars in CS80 sustained up to 65% higher strain demands than those in CS60 at the same drift levels. Up to a drift ratio of 1.5% and prior to bond failure, CS100 had twice the strains in the longitudinal bars as CS60 at the same drift levels. As the low-cycle fatigue life of reinforcing bars is related to experienced strain though a power function, a 100% increase in strain amplitudes can lead to an order of magnitude reduction in the number of cycles to fracture. Test results therefore raise concerns about the low-cycle fatigue life of HSRB in concrete members and the possible premature fracture of these bars during seismic events.
- Bond degradation initiated in CS100 beyond a drift ratio of 1.5%, which released the strains in longitudinal bars throughout the height of the member. Though columns had nearly identical flexural strength and associated shear demands, bond demands on longitudinal bars increased significantly with increasing steel strength. As the construction industry moves to higher-strength reinforcing bars, bond demands become more critical in designs. Currently, ACI 318-14 does not require an explicit check for the development length of longitudinal bars from points of maximum demand to points of flexural inflection. Test results indicate that the ACI 318-14 development length equations can be conserva-

tively used for this check. For well-confined columns satisfying ACI 318-14 SMF provisions, an increase on the cap of the confinement term in the ACI 318 development length relation from 2.5 to 3.0 may be applied. Due to potential damage in the plastic hinge regions, the effective available development length for longitudinal reinforcing bars in well-confined concrete columns sustaining inelastic deformations in their plastic hinge regions should not be taken larger than $((l/2) - (2/3)d)$.

AUTHOR BIOS

ACI member **Drit Sokoli** *is a Graduate Research Assistant at the University of Texas at Austin, Austin, TX, where he received his MS and is pursuing his PhD. He is a member of ACI Committee 369, Seismic Repair and Rehabilitation.*

ACI member **Wassim M. Ghannoum** *is an Assistant Professor at the University of Texas at Austin. He is Chair of ACI Committee 369, Seismic Repair and Rehabilitation, and a member of ACI Subcommittee 318-R, High-Strength Reinforcement (Concrete Building Code). His research interests include the behavior of reinforced concrete structures at high damage states and the life-span extension of concrete structures.*

ACKNOWLEDGMENTS

The authors wish to express their gratitude and sincere appreciation to Nucor Inc. Seattle and the Concrete Reinforcing Steel Institute (CRSI) for financing the research project.

NOTATION

A_g = gross sectional area of concrete member, in.^{2}
A_s = total area of longitudinal steel, in.^{2}
A_{tr} = total cross-sectional area of transverse reinforcing bars within spacing s that crosses potential plane of splitting, in.^{2}
a = length of shear span
b = width of section
c = $c_{min} + 0.5d_b$
c_b = smaller of: a) distance from center of bar to nearest concrete edge; and b) one-half center-to-center spacing between reinforcing bars, in.
c_{max} = maximum of (c_b, c_s)
c_{min} = minimum of (c_b, c_s)
c_s = minimum of (side cover, one-half clear spacing + 0.25)
d = effective section depth equal to distance from extreme compression fiber to centroid of outermost longitudinal tension reinforcement
d_b = diameter of reinforcing bar being developed or spliced, in.
E_c = modulus of elasticity of concrete, calculated as $57{,}000\sqrt{f_c'}$
f_c' = concrete compressive strength
f_{smax} = maximum stress during test in longitudinal bars determined from measured maximum strain and stress-strain relations determined from material testing
f_t' = tensile strength of concrete at day of testing and calculated as $7.5\sqrt{f_c'}$
f_y = measured yield strength of reinforcing bar
f_{yspec} = specified yield strength of reinforcing bar
h = length of section
k_{tr} = transverse reinforcement index
l = clear span of member
l_p = assumed plastic hinge length
M_{pr} = moment strength of section
n = number of reinforcing bars being spliced or developed along plane of splitting
s = spacing of transverse reinforcement
t_d = $0.78d_b + 0.22$, in.; term representing effect of bar size on contribution of transverse reinforcement to bond strength
V = column lateral load
V_e = peak design shear demand
V_{max} = maximum measured shear demand
V_s = steel contribution to shear strength
w = $0.1c_{max}/c_{min} + 0.9 \le 1.25$
ε_{cr} = concrete tensile strain at cracking
λ = modification factor equal to 1.4 reflecting reduced mechanical properties of lightweight concrete, or equal to 1.0 for normalweight concrete
ρ_l = ratio of area of distributed longitudinal reinforcement to gross concrete area perpendicular to that reinforcement
ρ_t = ratio of area distributed transverse reinforcement to gross concrete area perpendicular to that reinforcement
ψ_e = factor of 1.3 to account for epoxy-coated reinforcement, or equal to 1.0 for uncoated reinforcement
ψ_s = factor to account for size of reinforcing bars, equal to 0.8 for No. 6 (19 mm diameter) bars and smaller, or equal to 1.0 for No. 7 (22.23 mm diameter) bars and larger
ψ_t = reinforcement location factor equal to 1.3 for horizontal reinforcing bars with more than 12 in. (305 mm) fresh cast concrete below the reinforcement, or otherwise equal to 1.0

REFERENCES

1. ACI Committee 318, "Building Code Requirements for Structural Concrete (ACI 318-14) and Commentary (ACI 318R-14)," American Concrete Institute, Farmington Hills, MI, 2014, 519 pp.

2. AASHTO, "AASHTO LRFD Bridge Design Specifications," American Association of State Highway and Transportation Officials, Washington, DC, 2014, 2160 pp.

3. NIST, "Use of High-Strength Reinforcement in Earthquake-Resistant Concrete Structures (GCR 14-917-30)," NEHRP Consultants Joint Venture, National Institute of Standards and Technology, Gaithersburg, MD, 2014, 231 pp.

4. Sokoli, D., "Seismic Performance of Concrete Columns Reinforced with High Strength Steel," master's thesis, University of Texas at Austin, Austin, TX, 2014, 166 pp.

5. ATC-115, "Roadmap for the Use of High-Strength Reinforcement in Reinforced Concrete Design," Applied Technology Council, 2015, 197 pp.

6. Rautenberg, J. M.; Pujol, S.; Tavallali, H.; and Lepage, A., "Drift Capacity of Concrete Columns Reinforced with High Strength Steel," *ACI Structural Journal*, V. 110, No. 2, Mar.-Apr. 2013, pp. 307-318.

7. Restrepo, J. I.; Seible, F.; Stephan, B.; and Schoettler, M. J., "Seismic Testing of Bridge Columns Incorporating High-Performance Materials," *ACI Structural Journal*, V. 103, No. 4, July-Aug. 2006, pp. 496-504.

8. FEMA, "Interim Testing Protocols for Determining the Seismic Performance Characteristics of Structural and Nonstructural Components (FEMA-461)," Federal Emergency Management Agency, Washington, DC, 2007, 138 pp.

9. Sokoli, D.; Shekarchi, W.; Buenrostro, E.; and Ghannoum, W. M., "Advancing Behavioral Understanding and Damage Evaluation of Concrete Members Using High-Resolution Digital Image Correlation Data," *Earthquakes and Structures*, V. 7, No. 5, 2014, pp. 609-626. doi: 10.12989/eas.2014.7.5.609

10. ASTM C39/C39M-05, "Standard Test Method for Compressive Strength of Cylindrical Concrete Specimens," ASTM International, West Conshohocken, PA, 2005, 7 pp.

11. ASTM A370-14, "Standard Test Methods and Definitions for Mechanical Testing of Steel Products," ASTM International, West Conshohocken, PA, 2014, 50 pp.

12. ASTM E8/E8M-13, "Standard Test Methods for Tension Testing of Metallic Materials," ASTM International, West Conshohocken, PA, 2013, 29 pp.

13. Sezen, H., and Moehle, J. P., "Seismic Tests of Concrete Columns with Light Transverse Reinforcement," *ACI Structural Journal*, V. 103, No. 6, Nov.-Dec. 2006, pp. 842-849.

14. Ghannoum, W. M., and Moehle, J. P., "Shake-Table Tests of a Concrete Frame Sustaining Column Axial Failures," *ACI Structural Journal*, V. 109, No. 3, May-June 2012, pp. 393-402.

15. Ghannoum, W. M., and Moehle, J. P., "Dynamic Collapse Analysis of a Concrete Frame Sustaining Column Axial Failures," *ACI Structural Journal*, V. 109, No. 3, May-June 2012, pp. 403-412.

16. Brown, J., and Kunnath, S. K., "Low-Cycle Fatigue Failure of Reinforcing Steel Bars," *ACI Materials Journal*, V. 101, No. 6, Nov.-Dec. 2004, pp. 457-466.

17. Slavin, C. M., "Defining Structurally Acceptable Properties of High-Strength Steel Bars through Material Testing," master's thesis, University of Texas at Austin, Austin, TX, 2015, 136 pp.

18. LeBorgne, M., and Ghannoum, W., "Calibrated Analytical Element for Lateral-Strength Degradation of Reinforced Concrete Columns," *Engineering Structures*, V. 81, 2014, pp. 35-48. doi: 10.1016/j.engstruct.2014.09.030

19. LeBorgne, M., and Ghannoum, W., "Analytical Element for Simulating Lateral-Strength Degradation in Reinforced Concrete Columns and Other Frame Members," *Journal of Structural Engineering*, ASCE, V. 140, No. 7, 2014, pp. 04014031 1-12.

20. ASCE, "Seismic Evaluation and Retrofit of Existing Buildings (ASCE 41-13)," American Society of Civil Engineers, Reston, VA, 2013, 1074 pp.

21. ACI Committee 408, "Bond and Development of Straight Reinforcing Bars in Tension (ACI 408R-03)," American Concrete Institute, Farmington Hills, MI, 2003, 49 pp.

22. Ichinose, T., "Splitting Bond Failure of Columns under Seismic Action," *ACI Structural Journal*, V. 92, No. 5, Sept.-Oct. 1995, pp. 535-542.